Journal of Macromolecular Science, Part A
Publication details, including instructions for authors and subscription information:
http://www.informaworld.com/smpp/title~content=t713597274

pH- and Temperature-sensitive Nanoparticles Prepared using Salt Bridge

Xia Yang[a]; Hyeon Yong Lee[a]; Jin-Chul Kim[a]
[a] School of Biotechnology and Bioengineering and Institute of Bioscience and Biotechnology, Kangwon National University, Chunchon, Kangwon-do, Korea

To cite this Article Yang, Xia , Lee, Hyeon Yong and Kim, Jin-Chul(2009) 'pH- and Temperature-sensitive Nanoparticles Prepared using Salt Bridge', Journal of Macromolecular Science, Part A, 46: 10, 959 — 966
To link to this Article: DOI: 10.1080/10601320903158305
URL: http://dx.doi.org/10.1080/10601320903158305

Journal of Macromolecular Science®, Part A: Pure and Applied Chemistry (2009) **46**, 959–966

ISSN: 1060-1325 print / 1520-5738 online
DOI: 10.1080/10601320903158305

Taylor & Francis
Taylor & Francis Group

pH- and Temperature-sensitive Nanoparticles Prepared using Salt Bridge

XIA YANG, HYEON YONG LEE and JIN-CHUL KIM*

School of Biotechnology and Bioengineering and Institute of Bioscience and Biotechnology, Kangwon National University, 192-1, Hyoja 2-dong, Chunchon, Kangwon-do 200-701, Korea

Received March 2009, Accepted April 2009

Nanoparticles could be formed by salt bridges between the amino groups of poly (N-isopropylacrylamide-co-dimethylaminoethyl methacrylate) (P(NIPAM-co-DMAEMA)) and the carboxylic groups of fatty acids (FAs, stearic acid, palmitic acid, or lauric acid). FAs constitute the cores of nanoparticles and the copolymer stabilizes them. The colloidally stable nanoparticles could be obtained in the range of pH 6.0–9.0. Under strong acidic conditions (at pH 3.0 and 4.0), however, a marked increase in the size was observed. The pH values (3.0 and 4.0) were less than pK of the carboxylic acid of FAs, so the salt bridges will significantly decrease in number, resulting in the detachment of the copolymer from the surface of nanoparticles. Thus, an agglomeration due to hydrophobic interaction would be responsible for the size increase. The nanoparticles were pH-sensitive in terms of change in their sizes, due to the pH-sensitivity of the salt bridges. In addition, the sizes were also temperature-sensitive due to the temperature-dependent hydrophilicity of P(NIPAM-co-DMAEMA).

Keywords: Nanoparticles, salt bridges, pH-sensitive, temperature-sensitive

1 Introduction

Nanoparticles such as vesicles, polymeric micelles and solid lipid nanoparticles (SLNs) have been widely used in drug delivery systems. Nowadays, SLNs still have attracted the great interest of scientists. For instance, triptolide-loaded SLNs were reported to enhance the transdermal delivery and anti-inflammatory activity (1), and hinokitiol-containing SLNs which could enhance the permeation of hinokitiol were prepared using stearic acid by a melt-emulsification method (2). On the other hand, polymers having both hydrophilic and lipophilic segments could be self-assembled into polymeric micelles in aqueous phases (3, 4). Depending on the molecular structure and chemical composition of the polymer, the size ranges from tens to hundreds of nm. Most of polymeric micelles exhibit the structure of lipophilic core and hydrophilic shell (5, 6). In fact, hydrophilic segments constituting the shell prevent core-to-core interaction between nanoparticles and they act as a stabilizer (7, 8). The micelles can also be prepared using non-covalent interaction instead of chemical conjugation. For instance, the mixed micelles of poly(*N*-isopropylacrylamide)-*block*-poly(L-lactide) (PNIPMAM-*b*-PLLA) and poly(ethylene glycol)-*block*-poly(D-lactide) (PNIPAM-*b*-PDLA) formed through stereocomplexation were prepared by directly dissolving the two polymers in deionized water. The formation of the micelles relies on the strong non-covalent interaction between the core-forming hydrophobic blocks (9). Additional micelles prepared by using poly(aspartic acid)-poly(ethylene glycol) (PASP-PEG) with anionic pendant groups and diminazene aceturate, a small molecular cationic drug, were formed through non-covalent interaction (10). In addition, nanoparticles with small sizes can avoid the clearance by reticuloendothelial system (RES) because the hydrophilic shells prevent the adsorption of plasma protein and the adhesion of cells, resulting in favorable delivery of anti-cancer drug to solid tumors (11–13).

Moreover, hydrophobically modified PNIPAM was used for the preparation of thermoresponsive nanoparticles (14–16). Terminal-incorporated hydrophobic groups formed hydrophobic domains and PNIPAM segments formed hydrophilic outer layers (17). When the temperature increased across the lower critical solution temperature (LCST) of PNIPAM, the polymers are dehydrated and they become hydrophobic. Hence, the outer shell of the nanoparticles will collapse which could induce the deformation of core-shell structures. As a result, the drug

*Address correspondence to: Jin-Chul Kim, School of Biotechnology and Bioengineering and Institute of Bioscience and Biotechnology, Kangwon National University, 192-1, Hyoja 2-dong, Chunchon, Kangwon-do 200-701, Korea. Tel.: +82 33 250 6561; Fax: +82 33 253 6560; E-mail: jinkim@kangwon.ac.kr

molecules will be exposed to the external release medium (18, 19). The diffusion rate will also be accelerated with a higher temperature. On the other hand, pH-responsive nanoparticles were prepared using pH-sensitive dimethylaminoethyl methacrylate (DMAEMA) or methacrylic acid (MAA). The pH-response phenomena were obtained because of the deionization and ionization of carboxylic groups in MAA or amino groups in DMAEMA (20–23).

In this study, nanoparticles were prepared by taking advantage of a salt bridge formed between copolymer of NIPAM and DMAEMA, and fatty acids (FAs). The carboxylic groups of negative charge in the FAs will be electrostatically attached to amino groups of positive charge in DMAEMA residues. Thus, the FAs constitute the cores of nanoparticles and the copolymer stabilizes them. It is reported that cationic vesicles composed of fatty acid and N-[3-(dimethylamino)propyl]-octadecanamide were successfully prepared by salt bridge which will be broken down at acidic pH (24). However, there is no previous research about polymeric micelles formed by salt bridge. Three kinds of FAs (stearic acid (SA), palmitic acid (PA) and lauric acid (LA)) were used to investigate the effect of the hydrocarbon chain length on the formation of nanoparticles. Transmission electron microscopy (TEM) by a negative staining technique was employed to find out which kinds of nanoparticles would be obtained with FAs having different chain length. In addition, critical association concentrations (CACs) were determined by measuring surface tensions. Furthermore, since the NIPAM copolymer is thermo-sensitive and the salt bridge between the copolymer and FAs is sensitive to pH change, the nanoparticles in our research were thought to be both pH- and temperature- sensitive. Hence, the pH- and temperature-responsive properties of the nanoparticles were observed in terms of change in sizes on a particle size analyzer.

2 Experimental

2.1 Materials

Monomer of N-isopropylacrylamide (NIPAM, M.W. 113.16) was purchased from Tokyo Chemical Industry CO. (TCI, Tokyo, Japan) and dimethylaminoethyl methacrylate (DMAEMA, M.W. 157.22) was purchased from Sigma (St. Louis, USA). α,α'-Azobis(isobutyronitrile) (AIBN, M.W. 164.21) was purchased from Junsei Chemical CO., Ltd. (Tokyo, Japan). Fatty acids (FAs) used in this study were stearic acid (SA, M.W. 284.48), palmitic acid (PA, M.W. 256.4) and lauric acid (LA, M.W. 200.3) obtained from Sigma (St. Louis, USA). 4-(2-hydroxyethyl)-1-piperazineethanesulfonic acid (HEPES, M.W. 238) was purchased from Sigma (St. Louis, USA). All other reagents were in analytical grade.

2.2 Preparation and Characterization of NIPAM/DMAEMA Copolymers

Copolymer of NIPAM/DMAEMA (P(NIPAM-co-DMAEMA)) were prepared by a free radical reaction (25). The molar ratio of NIPAM/DMAEMA monomer was 95/5. The lower critical solution temperature (LCST) was observed by measuring the turbidities of copolymer solution in HEPES buffer (10 mM, pH 6) at 600 nm on a UV spectrophotometer (6505 UV/Vis. Spectrophotometer, JENWAY, U.K) equipped with a temperature controller. The concentration of the solution was adjusted to 20 mg/ml and the temperature was raised from 25°C to 45°C at a rate of 2°C/min.

2.3 Preparation of FAs/P(NIPAM-co-DMAEMA) Nanoparticles

FAs/P(NIPAM-co-DMAEMA) micelles were prepared by a dialysis method (26). 115.37 mg of copolymers (0.05 mol of DMAEMA) and variable amounts of FAs (0.01 mol) were dissolved in 2 ml ethanol so that the molar ratio of FA to DMAEMA was 1:5. The solution was put into 20 ml of HEPES buffer (pH 6.0, 10 mM) and then the mixture was stirred for 10 min. The mixture was put in a dialysis bag (MWCO 50,000) and it was dialyzed against 1000 ml of HEPES buffer (10 mM, pH 6.0) for 24 h with 6 times exchanges of the buffer. The final concentration of particles was adjusted to 5 mg/ml.

2.4 Transmission Electron Microscopy (TEM) and Size Distributions

The morphology of the FAs/P(NIPAM-co-DMAEMA) particles were investigated on TEM (LEO-912AB OMEGA, LEO, Germany) using a negative staining method (27). The size distributions of particles were carried out using a particle size analyzer (Plus 90, Brookhaven, USA) at pH 6, 25°C.

2.5 Surface Tension Measurement

Critical association concentrations (CACs) were determined by a surface tension method (28). FAs/P(NIPAM-co-DMAEMA) or P(NIPAM-co-DMAEMA) was dissolved in HEPES buffer (10 mM, pH 6.0) at various concentrations. Measurements were made using a ring method with a tension meter (SEO D60A, Korea). For pH-dependent surface tension measurement, the pHs were adjusted from 3 to 9. The concentration was fixed to 0.001 mg/ml. All the measurements were repeated 3 times under a specific condition, and the values were averaged.

2.6 pH-dependent Particle Sizes and Zeta Potentials

The particle sizes and zeta potentials were measured at various pHs (pH 3.0-pH 9.0) on a particle size analyzer (Plus 90, Brookhaven, USA) at 20°C. When the effect of temperature on the size was observed, the temperature was raised from 20 to 45°C, keeping the pH of medium at 6.0. In order to investigate the reversibility of temperature-dependent variation in size, the suspensions were cooled down to 20°C after heating to 45°C, and the size was measured again at 20°C.

3 Results and Discussion

3.1 Transmission Electron Microscopy and Size Distributions

Figure 1 shows TEM photos of FAs/P(NIPAM-co-DMAEMA) particles in HEPES buffer (10 mM, pH 6, 25°C). The particles of SA/P(NIPAM-co-DMAEMA) were almost spherical and the size was hundreds of nanometers (Fig. 1a). It is believed that the particles are solid lipid nanoparticles (SLN) stabilized with the copolymer. In fact, SA was well known to form SLN with aid of a stabilizer (29). On the other hand, the particles of PA/P(NIPAM-co-DMAEMA) were not strictly spherical and the size was less than that of SA/P(NIPAM-co-DMAEMA) (Fig. 1b). Since there a lot of particles found which size is tens of nanometers, polymeric micelles were thought to be formed together with SLN (the definition of size for polymeric micelle is from 20 to 100 nm (7)). When P(NIPAM-co-DMAEMA) and FA are dispersed in an aqueous system, there will be two major interactions which determine the shape and the size of particles. One is an electrostatic interaction between FA and P(NIPAM-co-DMAEMA), and the other is a hydrophobic interaction among FA molecules. The carboxylic groups of FA will electrostatically interact with the amino groups of P(NIPAM-co-DMAEMA) to form a salt bridge. Accordingly, FA will be attached to the copolymer along the backbone, leading to the formation of a polymeric amphiphiles (FA-attached P(NIPAM-co-DMAEMA)). The polymeric amphiphiles could form micelles and they could also be a stabilizer for SLN. On the other hand, the hydrophobic interaction among FA molecules will result in the formation of SLN. In case of SA, the hydrophobic interaction among SA molecules would prevail over the electrostatic interaction between SA and P(NIPAM-co-DMAEMA), due to its longer hydrocarbon chains. This may explain the formation of SLN in Figure 1a. Compared with SA, the hydrophobic interaction among PA molecules will be weaker due to its shorter hydrocarbon chains, but the electrostatic interaction between PA and P(NIPAM-co-DMAEMA) will be more significant. Accordingly, the formation of PA-attached P(NIPAM-co-DMAEMA) could be more favorable than that of SA-attached copolymer, leading to the favorable formation of polymeric PA micelles. Therefore, polymeric micelles are believed to be formed along with SLN when PA was used in the preparation. The particles of LA/P(NIPAM-co-DMAEMA) are shown in Figure 1c. The particles were much smaller that those of SA/P(NIPAM-co-DMAEMA) and PA/P(NIPAM-co-DMAEMA). The hydrophobic interaction among LA molecules will be much weaker due to its shorter hydrocarbon chains, but the electrostatic interaction between LA and P(NIPAM-co-DMAEMA) will be more pronounced, leading to the more favorable formation of LA-attached P(NIPAM-co-DMAEMA). In fact, a significant portion of the particles shown in Figure 1c looks like polymeric micelles. In addition, since FA having a shorter hydrocarbon chain (e.g. LA) would be surface-active due to a higher hydrophilic-lipophilic balance, it may be located at the interface of core and shell of the nanoparticles even without its attachment to the copolymer.

Figure 2 shows the size distributions of FAs/P(NIPAM-co-DMAEMA) particles in HEPES buffer (10 mM, pH 6, 25°C). The sizes of SA/P(NIPAM-co-DMAEMA) particles were 260–440 nm (Fig. 2a). Due to the longer hydrophobic chain of SA, as described in TEM photos, the hydrophobic aggregation of SA molecules will dominate the electrostatic interaction between SA and P(NIPAM-co-DMAEMA). Thus, SA SLN stabilized by SA-attached P(NIPAM-co-DMAEMA) seems to be responsible for the size distribution. The typical size of SA SLN was reported to be hundreds of nanometers (29). In the case of using PA and LA, there were two peaks in the size distributions. The sizes of PA/P(NIPAM-co-DMAEMA) particles were 80–150 nm and 210–320 nm (Fig. 2b). The sizes of LA/P(NIPAM-co-DMAEMA) particles were 20–90 nm and 190–280 nm (Fig. 2c). The populations located in the range of smaller sizes could come from polymeric micelles composed of FA-attached P(NIPAM-co-DMAEMA). The populations in the range of larger sizes may be due to SLN stabilized by FA-attached P(NIPAM-co-DMAEMA). When FAs having shorter hydrocarbon chains were used, the hydrophobic interaction among FA molecules will be suppressed and, instead, the electrostatic attachment of FA to P(NIPAM-co-DMAEMA) will be promoted, resulting in the favorable formation of polymeric micelles. As a result, the intensity of nanoparticles decreased and that of micelles increased when LA was used instead of PA (Fig. 2c).

3.2 Surface Tension Measurement

Figure 3 shows the surface tension of P(NIPAM-co-DMAEMA) solutions and FAs/P(NIPAM-co-DMAEMA) solutions at variable concentrations in HEPES buffer (10 mM, pH 6.0, 25°C). Whether FAs were added to the copolymer or not, the surface tension

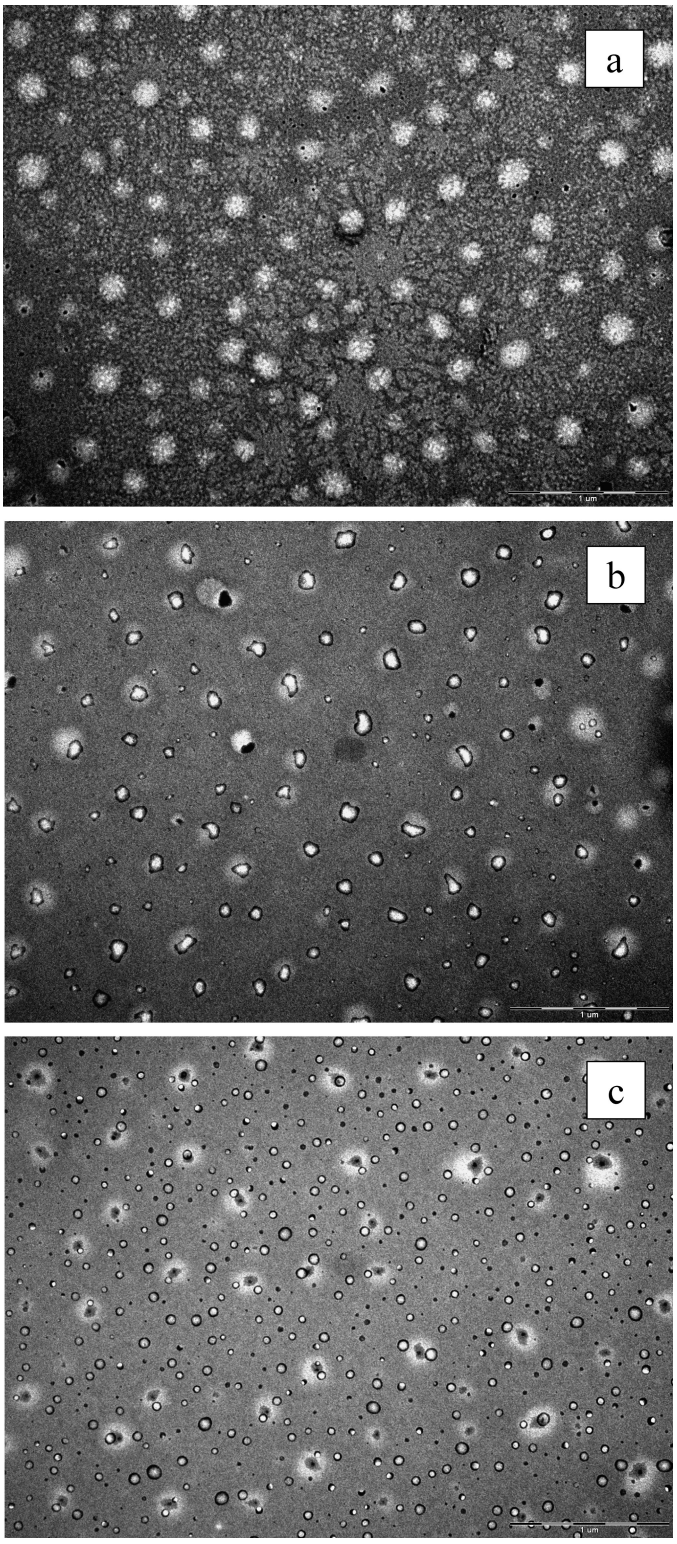

Fig. 1. TEM photos of FAs/P(NIPAM-co-DMAEMA) particles. (a) SA, (b) PA, (c) LA. The bars are 1000 nm.

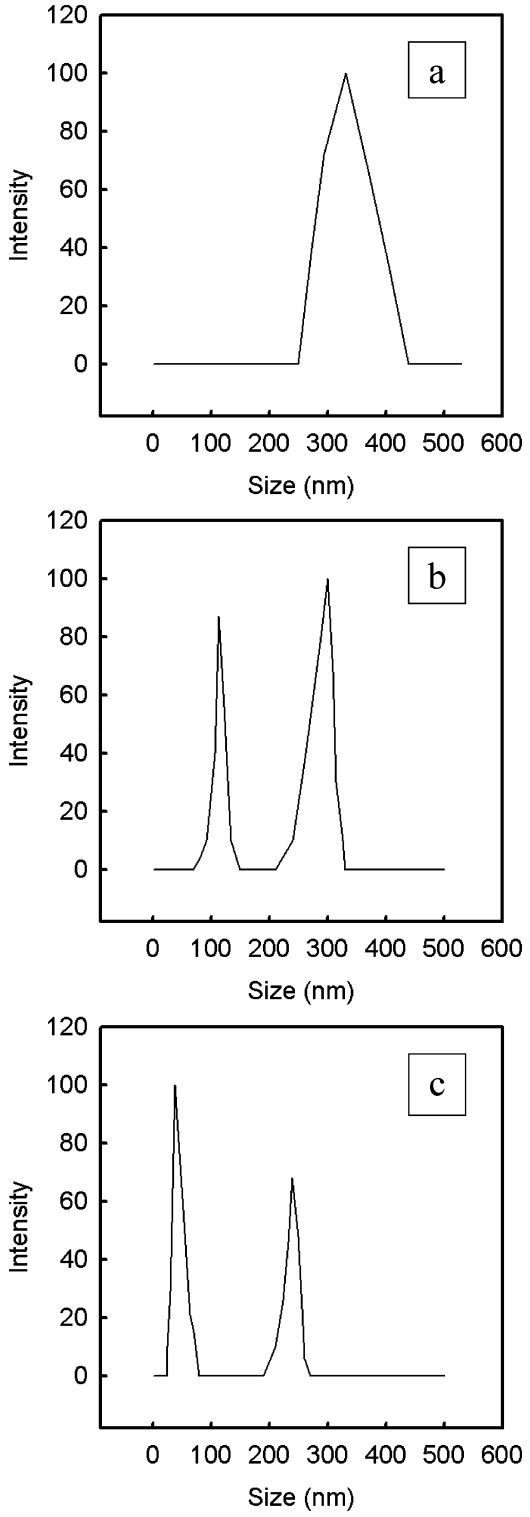

Fig. 2. Size distributions of FAs/P(NIPAM-co-DMAEMA) particles in HEPES buffer (10 mM, pH 6, 25°C). (a) SA, (b) PA, (c) LA.

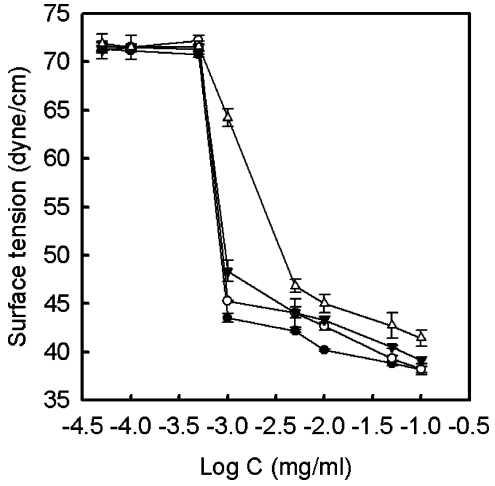

Fig. 3. Surface tension of P(NIPAM-co-DMAEMA) (△) solutions and FAs/P(NIPAM-co-DMAEMA) (SA (●), PA (○), LA (▼)) solutions at variable concentrations in HEPES buffer (10 mM, pH 6, 25°C).

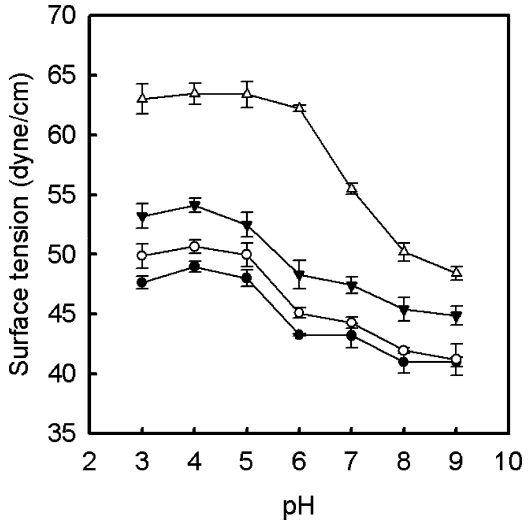

Fig. 4. Surface tension variations of P(NIPAM-co-DMAEMA) (△) solutions and FAs/P(NIPAM-co-DMAEMA) (SA (●), PA (○), LA (▼)) solutions with pH in HEPES buffer (10 mM, 25°C). The concentrations were 0.001 mg/ml.

markedly decreased by adding a small amount of P(NIPAM-co-DMAEMA). At the concentrations less than 0.001 mg/ml (fourth data points), the effect of FAs on the surface tension was negligible, where the value of surface tension was almost the same for all the samples (71–72 dyne/cm). At the concentration of 0.001 mg/ml and above, the effect of FAs became pronounced. For example, at the concentration of 0.001 mg/ml, the surface tension of the copolymer solution without FAs was 64.22 ± 0.894 dyne/cm, and those of the copolymer with FAs (LA, PA and SA) were 48.36 ± 1.110, 45.28 ± 0.042 and 43.52 ± 0.467 dyne/cm, respectively. It indicates that the hydrophobic FA is attached to copolymers by a salt bridge, and FA brings them to air/water interface, leading to a reduced surface tension. Following the inflections in the curves, the CACs of copolymers with FAs (LA, PA and SA) were almost the same (about 0.001 mg/ml) under our experimental conditions. There was no apparent inflection in the curve of copolymer without FAs. However, the CAC of copolymer without FA is around 0.005 mg/ml, which is higher than the CAC of copolymer with FA. That means the attachment of FAs to the copolymer increased the hydrophobicity, leading to the formation of nanoparticles at a lower concentration.

Figure 4 shows the surface tension variations of P(NIPAM-co-DMAEMA) solutions and FAs/P(NIPAM-co-DMAEMA) solutions with pH at the concentration of 0.001 mg/ml. In the case of copolymers without FAs, the surface tension was almost constant (63 dyne/cm) with respect to pH ranging from 3 to 6 and the value decreased to 48 dyne/cm at pH 9. The reason why the surface activities of the copolymer are lower at lower pHs is that there is a titrable group, amino group, in the copolymer and it tends to be ionized at lower pHs. That means the copolymers will become more soluble at lower pHs resulting in losing their surface activities. The behaviors of pH-dependent surface activity of the copolymer with FAs were similar to that of the copolymer without FAs, but the copolymers with FAs were more surface-active than the copolymers free of FAs because of the hydrophobic FAs segments. Furthermore, the longer the hydrocarbon of FA was, the higher the surface activity was. Due to a higher hydrophobicity, FA having a longer hydrocarbon chain could bring FA-attached copolymer to air/water interfaces more efficiently.

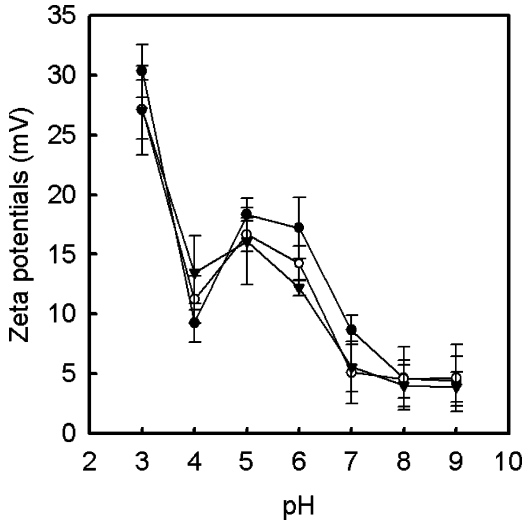

Fig. 5. pH-dependent zeta potentials of FAs/P(NIPAM-co-DMAEMA) particles (SA (●), PA (○), LA (▼)) in HEPES buffer (10 mM, 25°C).

3.3 pH-dependent Zeta Potentials and Particle Sizes

Figure 5 shows the pH-dependent zeta potentials of FAs/P(NIPAM-co-DMAEMA) particles. All the samples showed the positive charges in the full range of pH tested (pH 3–9). This is because the molar ratio of DMAEMA of the copolymer to FAs is 5 to 1. In other words, the number of positive charge is more than that of the negative charge. And the utmost layers of the particles would be the corona of the copolymer. Hence, the charge of the copolymer would determine the zeta potentials. This may explain why the surface is positively charged in the full range of pH tested. No significant difference in the zeta potentials of FAs/P(NIPAM-co-DMAEMA) particles was observed. For example, the potentials at pH 3 of FAs/P(NIPAM-co-DMAEMA) particles (SA, PA and LA) were +30.36 mV, +27.13 mV and +27.06 mV, respectively, and then the values dropped to about +4 mV at pH 8–9. Whether what kind of FA was used with P(NIPAM-co-DMAEMA), the surface compositions of FAs/P(NIPAM-co-DMAEMA) particles would be almost the same, because the copolymer was in excess with respect to FAs and accordingly the surfaces of the particles could be saturated with the copolymer. This could account for no significant difference in the zeta potentials of three kinds of particles. On the other hand, the zeta potential increased with decreasing pH in the range of pH 5.0–9.0. This is because the amino groups of P(NIPAM-co-DMAEMA) will be protonated with decreasing pH. A remarkable decrease of zeta potentials was observed when pH decreased from 5.0 to 4.0. The pK value of FAs is reported to be 4.5 to 5 (30). At pH 4.0, therefore, more than half of FA molecules will be unionized, and salt bridges between FA molecules and P(NIPAM-co-DMAEMA) will significantly decrease in number, possibly leading to the peeling-off of a significant amount of the copolymer from the surfaces of particles. As a result, the core of particles, FA, could be exposed. This could explain the marked decrease at pH 4.0. This phenomenon was also found in other research where the core of the micelle was exposed outside at pH 6.0–6.5 (31). The zeta potential increased again when the pH decrease from 4.0 to 3.0. At pH 3.0, the effect of ionization of the surface-attached copolymer on the zeta potential is likely to dominate over the effect of the peeling-off of the copolymer from the surface. Even though a small amount of copolymer would be adsorbed on the surface of nanoparticles at pH 3.0, the degree of ionization of the copolymer will be so high that the highest zeta potential is observed at pH 3.0.

Figure 6 shows pH-dependent size variations of FAs/P(NIPAM-co-DMAEMA) particles. In case of SA/P(NIPAM-co-DMAEMA) particles, the mean size was 320–390 nm at pH 6.0–9.0 and it dramatically increased to 990 nm as pH decreased to pH 3.0. The mean size of PA/P(NIPAM-co-DMAEMA) particle was 170–230 nm at pH 6.0–9.0 and it increased to 740 nm at pH 3.0. And for

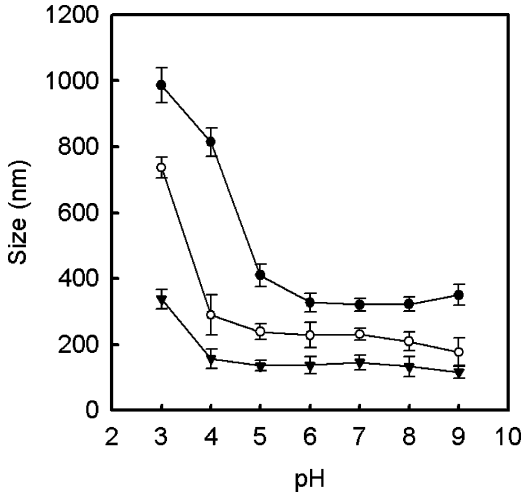

Fig. 6. pH-dependent particle sizes of FAs/P(NIPAM-co-DMAEMA) particles (SA (●), PA (○), LA (▼)) in HEPES buffer (10 mM, 25°C).

LA/P(NIPAM-co-DMAEMA) particles, the mean size was 110–140 nm at pH 6.0–9.0 and it increased to 340 nm at pH 3.0. At acidic conditions (pH < 4), most of carboxylic groups of FA will be unionized and a significant amount of the copolymer could be detached from the surfaces of FA particles. Thus, the particles could have a chance to aggregate by hydrophobic interaction, leading to an increase in size. In general, higher surface potentials result in higher repulsion among the nanoparticles, leading to large aggregates. Beside surface potentials, hydrophobic interactions will have a great effect on the aggregation of nanoparticles because the core of the nanoparticles is composed of hydrophobic FA. Even though the surface potential is the highest at pH 3.0 (Figure 5), the copolymer shell-free surface would be created since lots of copolymers could be detached from the surface of nanoparticles at pH 3.0. As a result, the nanoparticles could aggregate into large aggregates by hydrophobic interaction because the bare surfaces of nanoparticles are hydrophobic. This may account for why the size was the largest at pH 3.0 (Figure 6) even though the surface potential was the highest at the same pH (Figure 5).

When the pH of medium was 6.0–9.0, which are greater than pK of the carboxylic group and less than pK of the amino group, more than 50% of FA and P(NIPAM-co-DMAEMA) will be ionized. Accordingly, salt bridges between FA molecules and the copolymer will be readily formed and polymeric corona will surround the cores of nanoparticles (either polymeric micelles or lipid nanoparticles). The hydrophilic polymeric corona is likely to prevent the agglomeration of the nanoparticles, keeping the size almost constant in the range of pH 6.0–9.0.

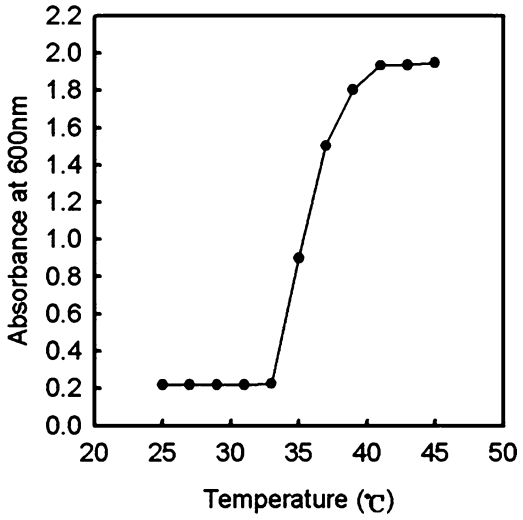

Fig. 7. Temperature-dependent turbidity of P(NIPAM-co-DMAEMA) solution in HEPES buffer (10 mM, pH 6). The concentration of copolymer was 20 mg/ml.

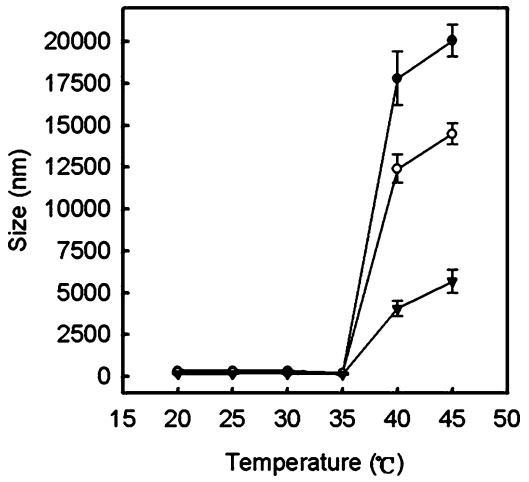

Fig. 8. Temperature-dependent particle sizes of FAs/P(NIPAM-co-DMAEMA) particles (SA (●), PA (○), LA (▼)) in HEPES buffer (10 mM, pH 6).

3.4 Temperature-dependent Particle Size

Figure 7 shows the temperature-dependent turbidities of P(NIPAM-co-DMAEMA) solution in HEPES buffer (pH 6.0). The copolymer solution was transparent at room temperature and it started to be turbid around 34°C. This is because the copolymer becomes hydrophobic and insoluble at its LCST. The LCST of the copolymer is a temperature slightly higher than that of homo PNIPAM (32°C). The copolymerization of NIPAM with hydrophilic monomers increases LCST (17). Since DMAEMA has ionizable amino groups and it is hydrophilic, a higher temperature was needed to change the copolymers from hydrophilic to hydrophobic form. This is account for why the LCST is higher when DMAEMA is copolymerized with NIPAM. On the other hand, the copolymers were reported to be mixtures which contained DMAEMA-rich copolymers produced in the early stage of reaction and NIPAM-rich copolymers in the latter stage due to the reactivity difference between NIPAM and DMAEMA (32). This may explain why the change of temperature-dependent turbidity was observed over somewhat broad temperature range, form 34°C to 40°C.

Figure 8 shows the temperature-dependent mean size of FAs/P(NIPAM-co-DMAEMA) particles in the range of 20 to 45°C. All the samples showed almost constant sizes in the range from 20 to 35°C due to the hydrophilic P(NIPAM-co-DMAEMA) shell. The hydrophilic polymeric shell could prevent the inner core interaction and stabilize the particles in suspension. Although the phase transition of the copolymers took place around 34°C (Fig. 7), the dehydration of the copolymer just above the temperature (e.g. 35°C), which is a prerequisite for the aggregation of the nanoparticles at the same temperature, is thought to be not enough to induce the hydrophobic interaction of the nanoparticles. This may be the reason why the size was unchanged at 35°C. The degree of dehydration increases with temperature so the hydrophobic interaction would readily occur at a higher temperature such as 40°C (Figure 8). Further heating from 35 to 45°C induced a significant increase in the particle size. The mean sizes increased from about 100–300 nm to more than tens of microns for particles containing SA and PA, and about 6000 nm for particles containing LA. Upon increasing temperature across LCST, the copolymers become hydrophobic. Accordingly, the hydrophobic interaction would be induced due to the increased hydrophobicity of the outer polymeric shell of particles, resulting in a size increase. Moreover, the mean sizes of all samples after cooling down were almost the same as those before heating (data is not shown here). This indicates that aggregates formed by heating can be re-dispersed upon cooling down to a temperature below the LCST. The reversibility is due to the re-hydration of the polymeric shell below the LCST.

4 Conclusions

Nanoparticles could be formed by electrostatically attaching anionic FAs to cationic water soluble copolymer (P(NIPAM-co-DMAEMA)). Depending on which FA (SA, PA, or LA) was used, lipid nanoparticles or both lipid nanoparticles and polymeric micelles could be obtained. The nanoparticles were pH-sensitive in terms of change in their sizes, due to the pH-sensitivity of salt bridges formed between FA and the copolymer. In addition, they were also temperature-sensitive in terms of change in sizes because of the temperature-dependent variation in hydrophilicity of P(NIPAM-co-DMAEMA).

Acknowledgements

This work was supported by a grant (20070401034013) from BioGreen 21 Program, Rural Development Administration, Republic of Korea.

References

1. Mei, Z., Li, X., Wu, Q., Hu, S. and Yang, X. (2005) *Pharmacol. Res.*, 51, 345–351.
2. Cho, S.M., Lee, H.Y. and Kim, J.C. (2007) *J. Am. Oil Chem. Soc.*, 84, 859–863.
3. Liu, C., Ni, P., Fang, X. and Zhou, X. (2009) *Colloid Polym. Sci.*, 287, 45–55.
4. Miguel, V.S., Limer, A.J., Haddleton, D.M., Catalina, F. and Peinado, C. (2008) *Eur. Polym. J.*, 44, 3853–3863.
5. Kataoka, K., Harada, A. and Nagasaki, Y. (2001) *Adv. Drug Deliv. Rev.*, 47, 113–131.
6. Li, G., Shi, L., An, Y., Zhang, W. and Ma, R. (2006) *Polymer*, 47, 4581–4587.
7. Wei, H., Zhang, X.Z., Zhou, Y., Cheng, S.X. and Zhou, R.X. (2006) *Biomaterials*, 27, 2028–2034.
8. Rieger, J., Passirani, C., Benoit, J.P., Butsele, K.V., Jérôme, R. and Jérôme, C. (2006) *Adv. Funct. Mater.*, 16, 1506–1514.
9. Kim, S.H., Tan, J.P.K., Nederberg, F., Fukushima, K., Yang, Y.Y., Waymouth, R.M. and Hedrick, J.L. (2009) *Macromolecules*, 42, 25–29.
10. Govender, T., Stolnik, S., Xiong, C., Zhang, S., Illum, L. and Davis, S.S. (2001) *J. Control. Release*, 75, 249–258.
11. Kwon, G.S. and Okano, T. (1996) *Adv. Drug Deliv. Rev.*, 21, 107–116.
12. Yokoyama, M., Okano, T., Sakurai, Y., Ekimoto, H., Shibazaki, C. and Kataoka, K. (1991) *Cancer Res.*, 51, 3229–3236.
13. Devalapally, H., Shenoy, D., Little, S., Langer, R. and Amiji, M. (2007) *Cancer Chemo. Pharm.*, 59, 477–484.
14. Choi, C., Chae, S.Y. and Nah, J.W. (2006) *Polymer*, 47, 4571–4580.
15. Chen, W.Q., Wei, H., Li, S.L., Feng, J., Nie, J., Zhang, X.Z. and Zhou, R.X. (2008) *Polymer*, 49, 3965–3972.
16. Loh, X.J., Zhang, Z.X., Wu, Y.L., Lee, T.S. and Li, J. (2009) *Macromolecules*, 42, 194–202.
17. Chung, J.E., Yokoyama, M., Aoyagi, T., Sakurai, Y. and Okano, T. (1998) *J. Control. Release*, 53, 119–130.
18. Chung, J.E., Yokoyama, M., Suzuki, K., Aoyagi, T., Sakurai, Y. and Okano, T. (1997) *Colloids Surf., B*, 9, 37–48.
19. Liu, S.Q., Tong, Y.W. and Yang, Y.Y. (2005) *Biomaterials*, 26, 5064–5074.
20. Liu, Y., Cao, X., Luo, M., Le, Z. and Xu, W. (2009) *J. Colloid Int. Sci.*, 329, 244–252.
21. Boudier, A., Aubert,-P.A., Louis,-P.P., Gérardin, C., Jorgensen, C., Devoisselle, J.M. and Bégu, S. (2009) *Biomaterials*, 30, 233–241.
22. Dufresne, M.H., Garrec, D.L., Sant, V., Leroux, J.C. and Ranger, M. (2004) *Int. J. Pharma.*, 277, 81–90.
23. Leroux, J.C., Roux, E., Garrec, D.L., Hong, K. and Drummond, D.C. (2001) *J. Control. Release*, 72, 71–84.
24. Kim, J.C., Song, M.E., Kim, M.J., Lee, E.J., Park, S.K., Rang, M.J. and Ahn, H.J. (2002) *Colloids Surf., B*, 26, 235–241.
25. Kono, K. (2001) *Adv. Drug Deliver. Rev.*, 53, 307–319.
26. Lee, E.S., Oh, K.T., Kim, D., Youn, Y.S. and Bae, Y.H. (2007) *J. Control. Release*, 123, 19–26.
27. Harris, J.R., Roos, C., Djalali, R., Rheingans, O., Maskos, M. and Schmidt, M. (1999) *Micron.*, 30, 289–298.
28. Shinoda, K., Yamaguchi, T. and Hori, R. (1961) *Bull Chem. Soc. Jpn.*, 34, 237–241.
29. Lee, J.H., Jung, S.W., Kim, I.S., Jeong, Y.I. and Kim, S.H. (2003) *Int. J. Pharma.*, 251, 23–32.
30. Kanicky, J.R. and Shah, D.O. (2003) *Langmuir*, 19, 2034–2038.
31. Wang, C.H., Wang, C.H. and Hsiue, G.H. (2005) *J. Control. Release*, 108, 140–149.
32. Hoare, T. and McLean, D. (2006) *Macromol. Theory Simul.,* 15, 619–632.